GOLD NANOPARTICLES MEDIATED TUNING OF THERMO-OPTICAL PARAMETERS IN GOLD NANOPARTICLES DOPED CHOLESTERIC LIQUID CRYSTAL NANOCOMPOSITE

G. Petriashvili [1], L. Devadze [1], Ts. Zurabishvili [1], N. Sepashvili [1], A. Chirakadze [1,2], T. Bukia [1], J. Markhulia [1], M. Areshidze [1], L. Sharashidze [1], Sh. Akhobadze [1], E. Arveladze [1], G. Sanikidze [1]

[1] Georgian Technical University
Vladimer Chavchanidze Institute of Cybernetics
Tbilisi, Georgia
g.petriashvili@yahoo.co.uk
devadze2005@yahoo.com
janomarkhulia@gmail.com
[2] Georgian Technical University
Engineering Physics Department
Tbilisi, Georgia
achikochirakadze@gmail.com

Accepted August 4, 2021

Abstract

Systems of nanoparticles (NPs) dispersed in liquid crystals (LCs) have attracted attention for the possible development of novel materials based on the controlled assembly of the NPs. There is investigated the formation of free-standing nanocomposites formed by the co-assembly of gold nanoparticles (GNPs) in the cholesteric liquid crystal (CLC) structures. It is found that increasing the concentration of GNPs in the CLC-mixture causes a significant modification of CLC structure and tuning of selective reflection band (SRB) over the optical spectrum. Furthermore, it is demonstrated that a light emission in the luminescent dye-doped CLC/GNPs-nanostructure can be increased dramatically when doped with a certain quantity of GNPs. The pumping laser beam onto the CLC/GNPs-nanostructure causes a temperature increase of this nanocomposite followed by SRB shifting of and spectral tuning of the stimulated laser emission lines from CLC/GNPs-nanocomposite.

Introduction

The new species of artificial composite substances often referred to as “metamaterials” have enormous potential for use in modern areas of science and technology. Especially noteworthy are the structures with nano-dimensions – nanoparticles (NPs) – which have unique optical and electro-optical properties and which differ significantly from the volumetric states created by the same substances.

It was found that the optical properties of metal nanoparticles (MNPs) depend mainly on their surface-plasmon resonance, where the term plasmon defines the collective oscillation of free electrons of MNPs. Surface plasmons can cause light absorption, scattering, and local field enhancement if there is an exciting light field. The plasmon resonance peak and the width of this peak are known to be sensitive to the size and shape of the MNPs, the type of metal, and the environment in which the NPs are placed.

Plasmonic MNPs have played a key role in this explosion of interest due to their capability of confining electromagnetic radiation at the nanoscale by exploiting a phenomenon called localized plasmonic resonance.

The noble metal NPs, gold and silver, exhibit particle plasmon resonances in the visible wavelength range **[1]**. Among MNPs, the study of gold nanoparticles (GNPs) has a special place because they have very interesting and attractive properties such as their organized distribution in different structures, electrical, magnetic, thermal and optical properties depending on the size, shape, concentration, etc. Driven by the utilization of these fascinating optical properties, GNPs have become one of the most remarkable areas of modern nanoscience and nanotechnology **[2, 3]**.

As is known, NPs can be incorporated into a variety of substances, such as metals, semiconductors, nuclear-membrane composites and organic polymers **[4, 5]**. Under this framework, research into micro/nano-scale colloids dispersed in liquid crystals (LCs) has facilitated enormous interest due to their potential scientific and technological relevance. The LCs form from organic compounds and are represented as the phase of condition between the solid and liquid states of a matter (**Figure 1**). For instance, a LC may flow like a liquid, but its molecules may be oriented in a crystal-like way. The LCs are characterized by the combination of partial ordering leading to anisotropic physical properties and fluidity, which allows control of molecular alignment by external stimuli such as temperature, light, magnetic, electric and acoustic fields, the influence of surfaces as well.

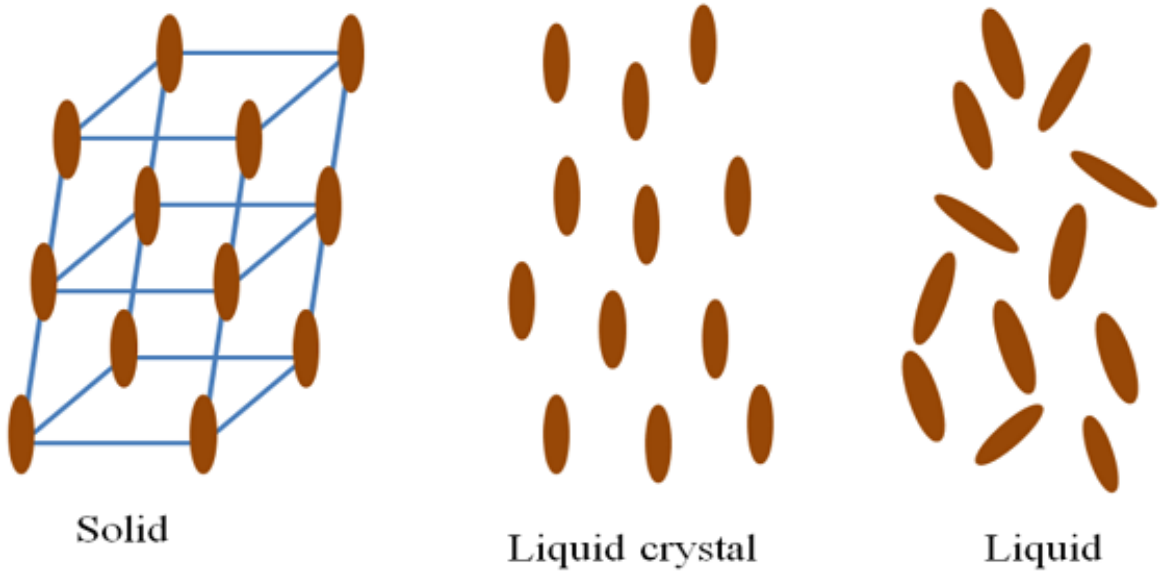

Figure 1. Solid, LC, and liquid states of matter.

And the greatest advantage of NPs-doped LCs is the rearrangement and management of the electro-optical and photo-optical properties of the NPs, which are fully consistent with the

 https://doi.org/10.52340/ns.2022.12

functional and structural labyrinth of the LCs. Experiments over the years have shown that NPs-coated LCs are distinguished by such electrical and photo-optical properties as enhanced photo-luminescence, reduced conduction voltages, fast reaction time and spontaneous vertical orientation of LCs. All this leads to the use of these substances in stimulated-response systems **[6 – 15]**.

Helical assemblies of NPs that combine a helical topology with the unique properties of NPs have been a research focus due to their applications in information storage, terahertz chiralplasmonic and biosensing **[16]**. It has been found that the properties of NPs-doped materials are significantly different from those of the host matrix **[17 – 19]**.

The cholesteric liquid crystal (CLC) phase is a nematic phase with a self-organized periodical helical arrangement that acts as a one-dimensional periodic structure **[20]**. The spiral, supramolecular structure of the CLC determines its many unique properties. When the helical pitch (period) coincides with the wavelength of the incident light, the distributed optical feedback gives selective reflectance and giant optical activity. Along the helical axis, the director is continuously rotated, which results in a twisted birefringent medium.

In CLCs the period of the structure is equal to half the pitch P of the helix, and for light propagating along the helical axes,

$$P_0 = \lambda_0 / n ,$$

where λ_0 is the wavelength of the maximum reflection or the middle of the selective reflection band (SRB) and n is the average of the refractive indices defined as

$$n = (n_E + n_O) / 2 ,$$

where the extraordinary and ordinary indices of refraction are denoted by n_E and n_O, respectively. The full width at half maximum of the SRB equals to

$$\Delta\lambda = P_0 \Delta n ,$$

where λ is the wavelength and

$$\Delta n = n_E - n_O$$

is the birefringence of a nematic layer perpendicular to the helix axis.

In this work, we have prepared a nanocomposite consisting of GNPs doped in a CLC-matrix and have shown that the GNPs can be dispersed in large quantities to the CLCs without the destruction of their structure. Besides, using the CLC doped with GNPs and luminescent dye, we have obtained a non-intrusive and controlled tuning of SRB of the CLC and demonstrated the enhancement and tuning of laser emissions from CLC/GNPs nanocomposite stimulated by the GNPs.

Materials and sample preparation

To prepare GNPs dispersed CLC nanocomposite, as the nematic host, it was chosen BL-090 ($\Delta n = 0.27$ at $\lambda = 589$ nm and temperature $T = 20°C$). And as the optically active dopant was chosen MLC-6248 with HTP (Helical Twisting Power) of 11.3 μm^{-1}. Both materials are available from Merck. As the nanomaterial, we used dodecylthiol functionalized GNPs, 10 nm, with the maximum of surface plasmon absorption at 520 nm (**Figure 2**) and to produce the desired output laser emission, a luminescent dye Nile red (NR) was used, both from Sigma–Aldrich (**Figure 3**).

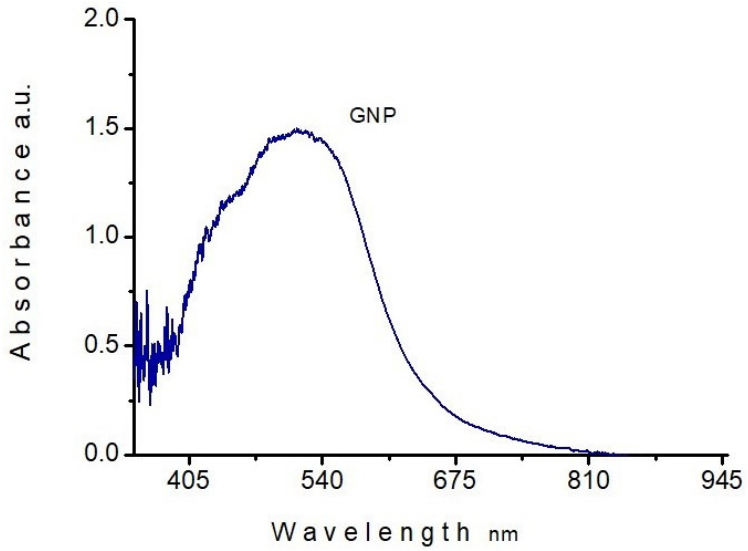

Figure 2. Surface plasmon absorption spectrum of 10 nm size GNPs.

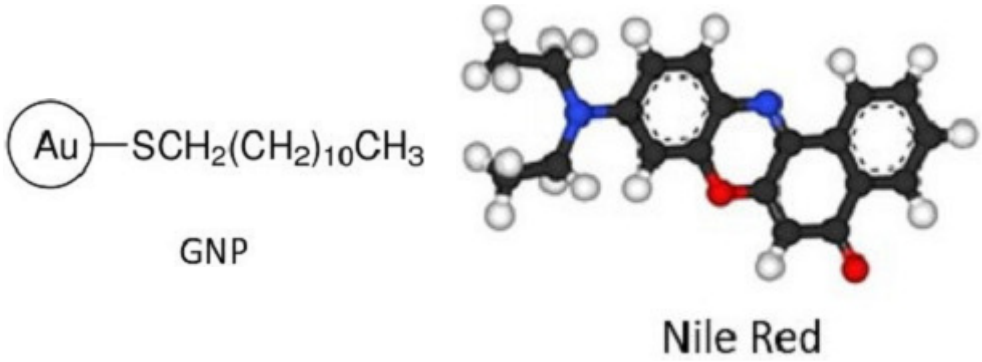

(a) **(b)**

Figure 3. Structural formulas of **(a)** GNP and **(b)** luminescent dye Nile red.

The CLC/GNPs nanocomposite was prepared by doping capped GNPs into CLC at the isotropic phase. The use of capped GNPs is very significant as the capping procedure controls the miscibility of GNPs into CLC, prohibits GNPs agglomeration in CLC, and maintains the long-lasting stability of CLC/GNP nanocomposite. The GNPs doped CLC mixture was prepared using BL-090, MLC-6248 and GNPs with the following concentrations in weight: [69.5%BL-090+ 30.5%MLC-6248]+X%GNPs, where X is the different concentration of GNPs doped in CLC mixture.

To investigate its thermo-optical properties, the CLC/GNPs nanocomposite was confined in a cell prepared with two glass plates. The spacing between the plates was set to 12 μm using the Mylar films. The surfaces of glass substrates were coated with Sigma–Aldrich PVA (PolyVinyl Alcohol). PVA was prepared in water at a concentration of 0.5% in weight. Thin layers of the PVA were deposited by spin-coating on glasses and rubbed to obtain planar alignment of the CLC material.

The samples were pumped with 7 ns pulses at 532 nm from a frequency-doubled Q-switched YAG:Nd (Yttrium Aluminum Garnet doped with Nd) laser. As the imaging-based technique was involved polarized optical and fluorescence microscopes equipped with high-resolution CCD (Charge-Coupled Device) cameras. A hot stage with 0.1°C accuracies was used to control the cell temperature. As the unpolarized and incoherent light source a conventional

 https://doi.org/10.52340/ns.2022.12

4 W quartz tungsten-halogen (QTH) lamp equipped with a collimating lens was used. The optical properties of the mixtures absorption, luminescence and reflection spectra, as the function of GNPs concentration and temperature, were investigated with a fiber-coupled spectrometer (Avantes, AvaSpec-2048) having 1 nm resolution.

GNPs concentration controlled tuning of SRB in CLC

The starting point of the experiment was to check how the system of CLC/GNPs evolves by gradually increasing the GNPs concentration in the CLC matrix. To obtain the CLC/GNPs nanocomposites next a mounts of GNPs material was added to the CLC mixture:

1. [69.5%BL-090+30.5%MLC-6248]+0%GNPs;
2. [69.5%BL-090+30.5%MLC-6248]+1%GNPs;
3. [69.5%BL-090+30.5%MLC-6248]+4%GNPs;
4. [69.5%BL-090+30.5%MLC-6248]+8%GNPs; and
5. [69.5%BL-090+30.5%MLC-6248]+12%GNPs.

The as-prepared solutions were vigorously stirred at 600 rpm for 12 h at room temperature to avoid aggregation and obtain homogeneous solutions. The GNPs conjugates were stable towards aggregation and under irradiation with visible blue, green and red lights. Using the spectrometer, we found that the positions of the SRBs of the doped mixtures are red-shifted by 160 nm to that of the pure CLC with $\lambda = 550$ nm, and the shift was approximately proportional to the GNPs concentration (**Figure 4**). However, it looks like a concentration threshold exists (about 13 – 14 wt.%), above which the CLC/GNPs nanocomposite contained in the optical cell does not show the selective reflection typical of CLC materials.

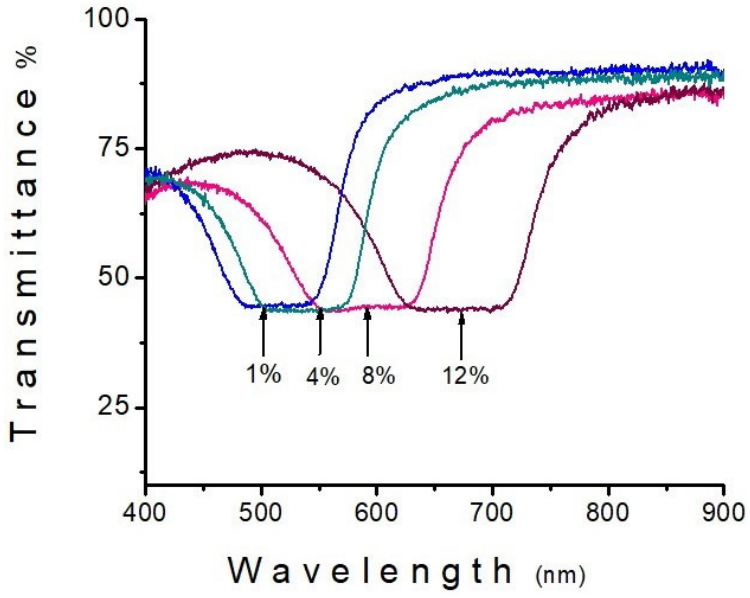

Figure 4. Tuning of SRB stimulated by varying of GNPs concentration in CLC/GNPs nanocomposite.

It is important to note that GNPs not just decorate the CLC structure, but are strongly conjugated with the CLC molecules experiencing specific interactions and create a novel helical structure with a larger pitch controlled by the concentration of GNPs. When a certain amount

of GNPs is doped in the CLC, the high field close to the GNPs can align individual CLC molecules surrounding the particles, forming the pseudo-CLC domains, where anisotropically shaped molecules exhibit short-range orientational order defined by a local director (**Figure 5**).

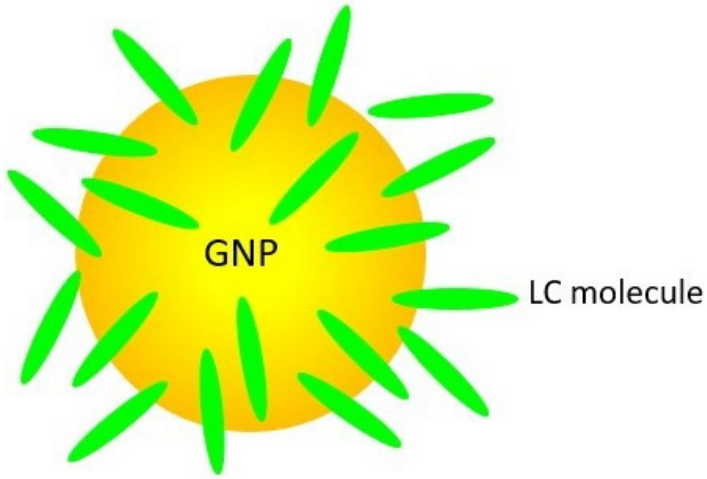

Figure 5. Schematic representation of NP-induced elastic distortions of liquid crystal molecules.

Using the polarized optical microscope we found that the GNPs have spatially self-assembled into the oily streaks of the disclination network of the CLC. The self-assembly of the GNPs into the defects is driven by the reduction of elastic free energy costs resulting from the stabilization of the CLC structure, which is in accordance with a minimum of energy condition associated with trapping of GNPs in a favorable area.

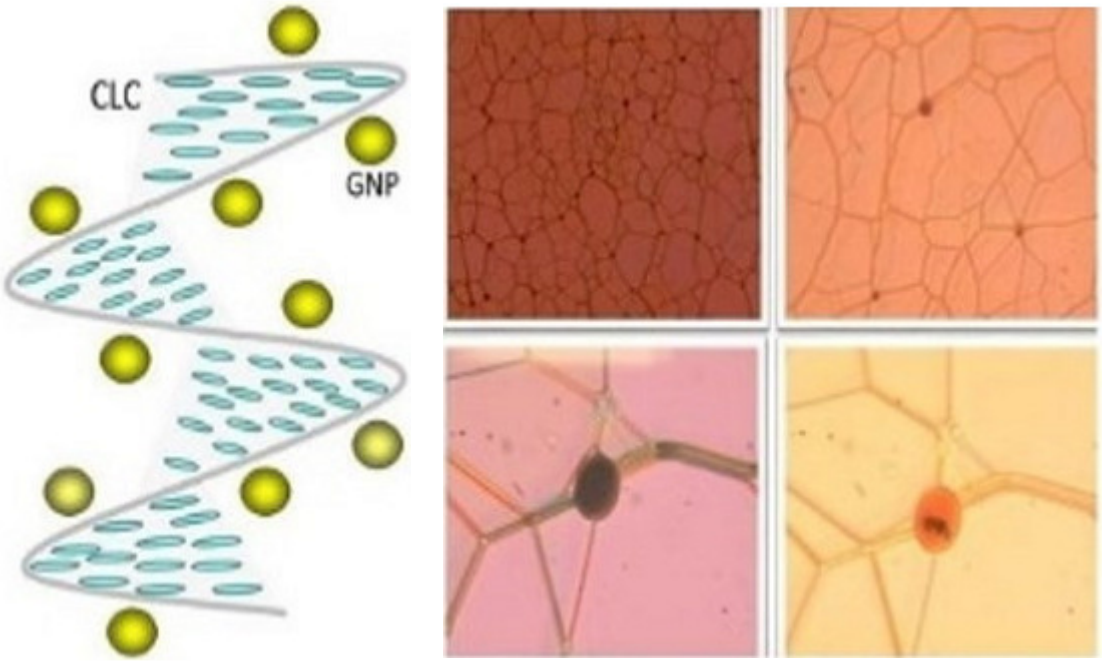

(a) **(b)**

Figure 6. Patterned GNPs in CLC structure: **(a)** schematic representation and **(b)** polarized optical microscopic image of clustered GNPs inside CLC disclination network.

 https://doi.org/10.52340/ns.2022.12

In this scenario, CLC acts as the 1D photonic structure stimulating the cooperative 1D self-assembly of GNPs into twisted helices (**Figure 6**).

In **Figure 7**, it is shown the image of CLC/GNPs nanocomposite with different concentrations of GNPs. In particular, **Figure 7a** displays 4%GNPs in weight dispersed in CLC structure, while **Figures 7b** and **7c** display the cases of 8 and 12% of GNPs concentrations in CLC, respectively.

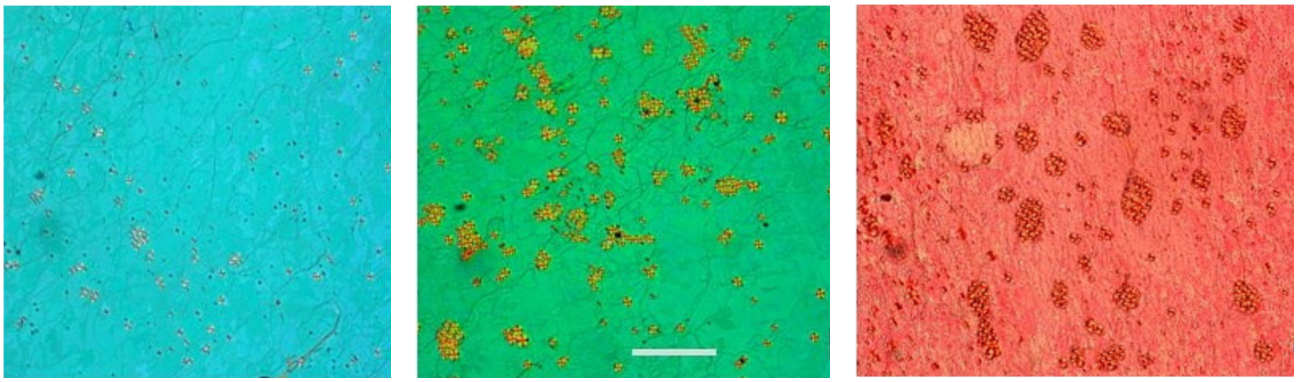

(a) **(b)** **(c)**

Figure 7. Optical polarized microscopic images of GNPs dispersed in CLC mixture with different concentration in weight: **(a)** 4%, **(b)** 8% and **(c)** 12%. Scale bar is 20 μm.

The introduction of GNPs in high concentrations in CLC will allow us to produce the LC structures based nanocomposites of different types and properties, which will significantly expand their areas of practical application.

The main results of the proposed research are:

(a) We have used a CLC as a host matrix, the period of SRB of which is located in the visible range of the optical spectrum and have continuously rearranged this period over the large spectral area; and

(b) Based on the innovative method developed by us, we have carried out an extremely large number of GNPs (their share is of ~12%) in CLC structures, so as not to aggregate (cluster) GNPs.

All this allows us to prepare qualitatively new types of nanocomposites and by varying the sizes, shapes, concentrations, positions and distances of GNPs it is possible obtain the appropriate structures to perform the set tasks.

Light-to-heat conversion in CLC/GNPs nanocomposite

GNPs can efficiently release heat under optical excitation conversion, which eventually is dissipated in the CLC environment through thermal convection.

Here we focus on the visualization of the optical energy conversion to heat caused in CLC/GNPs nanocomposite. When excited with a laser beam, the laser electric field strongly drives charge mobile carriers inside the GNPs, and the energy gained by the carrier turns into heat. Heat generation becomes especially strong in the regime of plasmon resonance **[21]**. The GNPs temperature may rise significantly and the heat can propagate to the surrounding medium.

In our method, the temperature surrounding the nanoparticles can be estimated by monitoring the spectral shift of the selective reflection peak of a CLC. As noted above, heat generation becomes especially strong in the case of plasmon resonance.

In the absence of phase transformations in the system, temperature field distribution around optically stimulated NPs is described by the standard heat transfer or the thermal diffusion equation:

$$P(\mathbf{r})\,C(\mathbf{r}) = \partial T(\mathbf{r},t)/\partial t =$$

$$= \Delta K(\mathbf{r})\,\Delta T(\mathbf{r},t) + Q(\mathbf{r},t)\,,$$

where **r** and t are space current point radius-vector and time current moment, respectively. T(**r**,t) is the local temperature; and the material parameters P(**r**), C(**r**) and K(**r**) are mass density, specific heat, and thermal conductivity, respectively. As for the function Q(**r**,t), it represents an energy source coming from light dissipation in nanoparticles:

$$Q(\mathbf{r},t) = J(\mathbf{r},t)\,E(\mathbf{r},t)\,,$$

where, J(**r**,t) is the current density and E(**r**,t) is the stimulating electric field in the system.

The heating effect can be strongly enhanced in the presence of a number of NPs. The accumulative effect comes from the addition of heat fluxes generated by single NPs and is described by the above stated thermal diffusion equation. The energy source in this equation should be written as a sum over all NPs:

$$Q(\mathbf{r},t) = \Sigma_k\, Q_k(\mathbf{r},t)\,,$$

where $Q_k(\mathbf{r},t)$ describes heat generation by the k-NP. The more NPs, the stronger the temperature increases that appears in the system.

GNPs stimulated tuning of SRB and laser lines in CLC/GNPs nanocomposite

In this section of the experiments, we have prepared and investigated the CLC/GNPs nanocomposite which acts as a thermo-chromic material with such improved parameters as temperature-controlled fine-tuning of SRB and laser emission upon the wide range of the optical spectrum.

To demonstrate the temperature-dependent tunable lasing from a CLC/GNP mixture, we used a [69.5%BL-090+30.5%MLC-6248]+12%GNPs nanocomposite doped with fluorescent NR. The optical cell was prepared and filled with CLC/GNPs/NR nanocomposite according to the above-mentioned procedures.

In **Figure 8**, there is shown a schematic of the experimental setup. The light emerging from the pumping laser propagates through the optical lens focusing the pumping beam into a spot with a diameter of 300 μm, which causes the local heating of CLC/GNPs nanocomposite and stimulating the spectral tuning of SRB of CLC structure.

On the other hand, the pumping beam stimulates the emission of laser lines from CLC/GNPs nanocomposite, which are shifted according to the tuning of SRBs of the CLC structure.

The spectral analysis is performed using a spectrometer.

 https://doi.org/10.52340/ns.2022.12

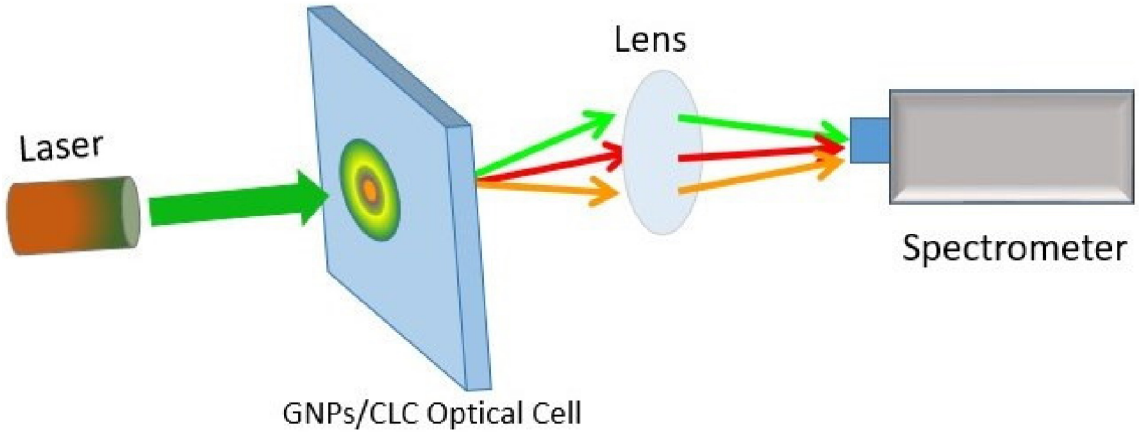

Figure 8. Schematic of experimental setup displays laser emission lines of CLC/GNPs nanocomposite pumped by 532 nm solid-state YAG:Nd laser.

The lasing performance of the samples was examined under optical excitation using a frequency-doubled pulsed YAG:Nd laser with a wavelength of 532 nm. The pulse duration was 8 ns with repetition rate of 10 Hz. A lens with 10 cm focal length was used to focus the emitted laser beams on the spectrometer.

Figure 9a shows a laser stimulated temperature-dependent tuning of SRB of CLC mixture, and **Figure 9b** demonstrates the laser line tuning from CLC/GNPs nanocomposite. Laser emissions were recorded at 629, 630, 594 and 579 nm, sequentially, which corresponds to the laser wavelength tuning range of about 51 nm.

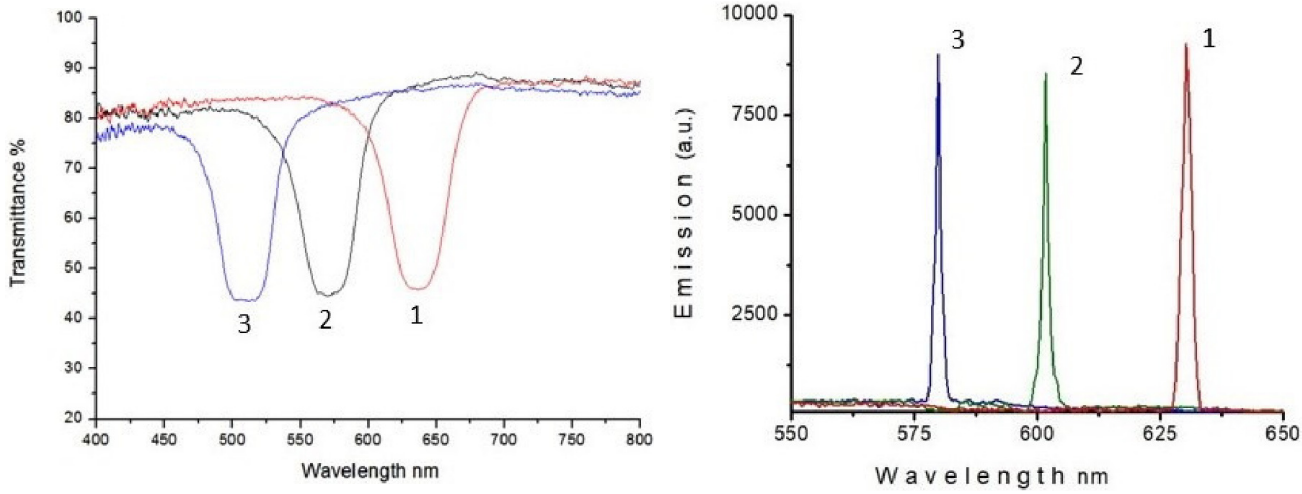

(a) **(b)**

Figure 9. Temperature-dependent shift of SRB together with effects of lasing tuning of emission wavelength.

GNPs stimulated light intensity enhancement in CLC/GNPs nanocomposite

Light incident on the GNPs induces the localized surface plasmon resonance (SPR), which stimulates the enhancement of the electromagnetic field on the GNPs surfaces.

Depending on the geometry of the absorbing materials (size, thickness, shape, etc.) and the coupling distance, the effect on the SPR can go from plasmon enhancement to complete quenching **[22]**. Here we show that when the GNPs surface SPR wavelength coincides with the wavelength of the excitation light source, the large optical fields provided by surface plasmons increase the fluorescence intensity of dye molecules by enhancing the molecular excitation rate.

Besides, we have observed a strong laser emission stimulated by GNPs. Two composites were prepared: one is the mixtures of CLC doped with 0.5% NR, and the other one is the CLC/GNPs nanocomposite doped with 0.5%NR:

1. [69.5%BL-090+30.5%MLC-6248]+0.5%NR; and
2. [69.5%BL-090+30.5%MLC-6248+4.0% GNPs]+0.5%NR.

A fluorescent microscope was used to examine the CLC/GNPs nanocomposites at a microscale. We note that under the experimental conditions an excitation wavelength of 532 nm coincides with the SPR peak of GNPs.

To investigate the light amplification stimulated by GNPs, we prepared two samples. The first one consists of CLC/NR composite, and the second one consists of CLC/GNPs/NR nanocomposite. Both samples were examined using a fluorescence microscope and then compared the images. A sample containing GNPs emits light much stronger than a sample that does not contain GNPs.

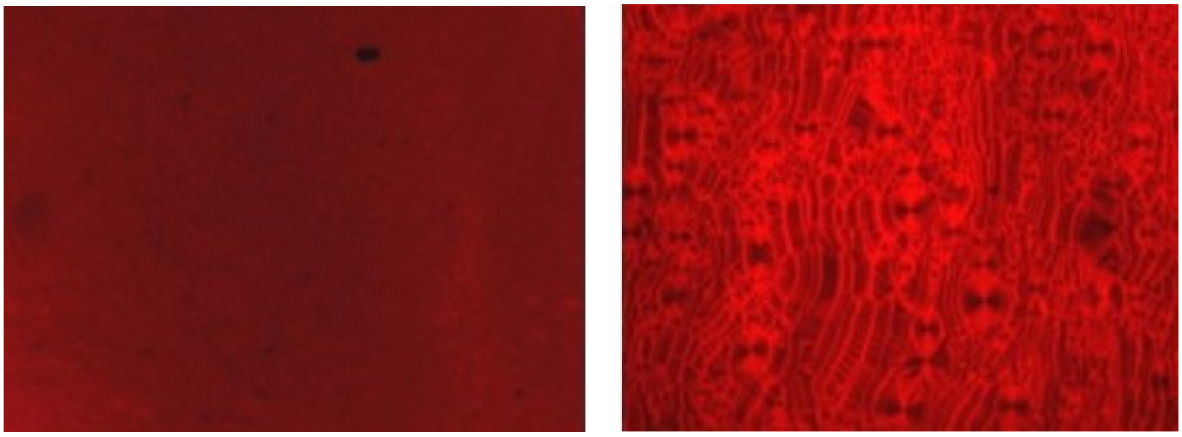

(a) **(b)**

Figure 10. Fluorescent microscopic images of **(a)** [69.5%BL-090+30.5%MLC-6248] +0.5%NR and **(b)** [69.5%BL-090 +30.5%MLC-6248 +4.0%GNPs] +0.5%NR composites.

Figure 10 shows the images of CLC/NR and CLC/GNPs/NR composites taken with fluorescence microscope: **Figure 10a** – the intensity of the light emitted by the CLC/NR composition and **Figure 10b** – the intensity of the light emitted by the CLC/GNPs/NR nanocomposite. First, the samples were irradiated from a QTH lamp equipped with a collimating lens and then samples were irradiated from pumped YAG:Nd laser.

As shown in **Figure 11a**, the fluorescence intensity emitted from 69.5%BL-090+ 30.5%MLC-6248+4.0%GNPs]+0.5%NR sample is stronger than the fluorescence intensity emitted from 69.5%BL-090+30.5%MLC-6248+0.5%NR sample. After that, composites were irradiated with YAG:Nd laser and was stimulated the laser emission in both samples. Here, too, the laser line emitted from CLC/GNPs/NR nanocomposite is much more intense than the laser line emitted from CLC/NR composite (**Figure 11b**).

 https://doi.org/10.52340/ns.2022.12

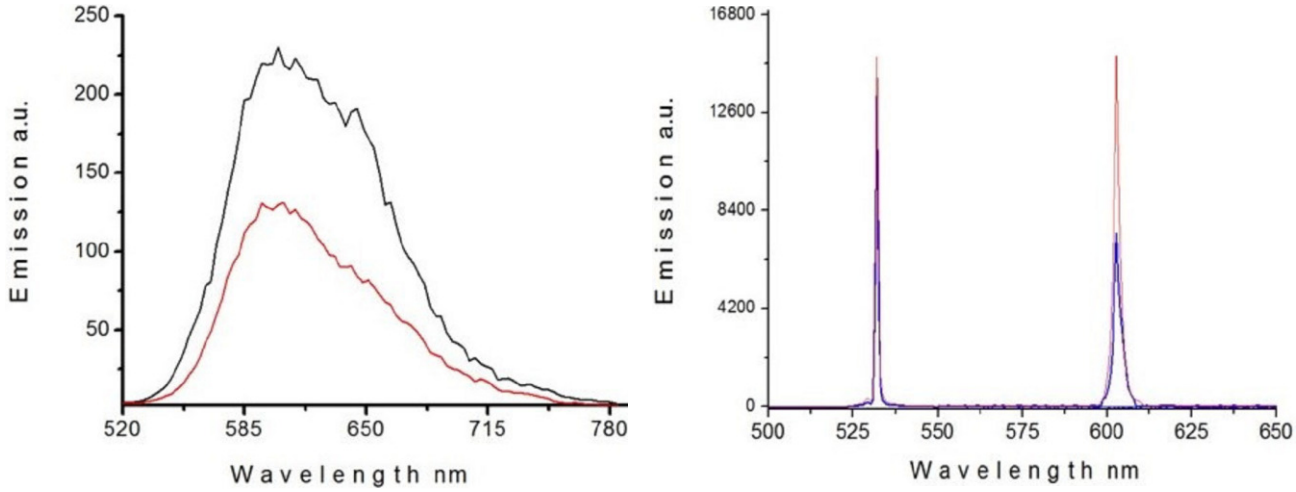

(a) (b)

Figure 11. Graphical illustration of **(a)** luminescent and **(b)** laser emissions in [69.5%BL-090+30.5%MLC-6248]+0.5%NR and [69.5%BL-090+30.5%MLC-6248+4.0%GNPs]+0.5%NR composites.

In the description of the nature of the energy transfer from an organic luminescence dye to a GNP, a crucial role plays the distance-dependence between the luminescence dye and the surface of a GNP. The altered electromagnetic field around the metal NP changes the properties of a dye that is placed in the vicinity.

It can cause two enhancement effects: the first is an increase in the quantum efficiency of the dye and the second is an increase in the excitation rate of the dye. The induced collective electron oscillations associated with the surface plasmon resonance, give rise to induce local electric fields near the NP surface.

Energy transfer from luminescent organic dyes to GNPs is generally considered to be the major process leading to the excited-state activation / deactivation of the dyes **[23]**. The most familiar mechanism is that of energy transfer via dipole–dipole interactions, i.e. FRET, from an energy donor to an energy acceptor. The energy transfer efficiencies E have been measured from the lifetime data using the following equation:

$$E = 1 - \tau / \tau_0 ,$$

where τ and τ_0 are the lifetimes of the donor in the presence and absence of the acceptor respectively. To determine a time-resolved luminescence, the luminescence lifetimes of the samples were measured as a function of time after being excited by a beam of light. A pulsed YAG:Nd laser with a wavelength of 532 nm was used to excite the CLC/GNPs nanocomposite. The induced electric field originating from the charge separation in the nanoparticle during the plasmon resonance oscillations is very large at very small distances from the surface. The dependence of the critical donor–acceptor distance R_0, when energy transfer efficiency is 50%, on the spectral overlap for a particular donor–acceptor pair is expressed as:

$$R_0 \approx 0.211 \, (K^2 \Phi_D J(\lambda) / N^4)^{1/6} ,$$

where K^2 represents the relative orientation of the donor to the acceptor molecule, considering a random rotational diffusion for the small molecules.

K^2 is taken to be 2/3 **[24]**. N is the refractive index of the medium (≈1.42 for CLC/GNPs nanocomposite), Φ_D is the quantum yield of the donor in the absence of the acceptor, taken as ≈ 0.43, and J(λ) is the overlap integral, which can be calculated from integration over the range (0, ∞) by the numerical method using the following relation:

$$J(\lambda) = \int d\lambda\, \lambda^4 F(\lambda)\, \varepsilon_A(\lambda) / \int d\lambda\, F(\lambda),$$

where $F(\lambda)$ is the luminescence intensity of the donor in the wavelength range $(\lambda, \lambda + \Delta\lambda)$ with the total intensity normalized to unity, $\varepsilon_A(\lambda)$ is the molar extinction coefficient of the acceptor.

For GNPs with 10 nm size (from Sigma–Aldrich) the molar extinction coefficient is equal to $1.01 \cdot 10^8$ $M^{-1} \cdot cm^{-1}$. The fact that GNPs have very large molar extinction coefficients makes them potentially excellent energy acceptors according to equation for R_0. The overlap integrals J(λ) for the present donor–acceptor were estimated to be ≈ $3.2 \cdot 10^{-6}$ $M^{-1} \cdot cm^3$. The energy transfer efficiencies in the thermal diffusion equation can be rewritten as:

$$E(r) = 1 / (1 + (r / R_0)^6).$$

According to the measured lifetime data for the energy transfer efficiencies from the corresponding formula we found E≈0.92. Finally, based on the experimental results and calculated data from the equations above stated system of equations, we found that the distance between the dye molecules and GNPs, which are statistically distributed in the polymer medium, is equal to 0.30 ± 0.15 nm.

Conclusion

We have designed and investigated a smart, stimuli-responsive CLC/GNPs based nano-platform, which can respond to endogenous and exogenous stimuli, such as NPs concentration, light, temperature, magnetic and electric fields, ultrasound.

Therefore, the obtained results can find applications in solar cells and concentrators, luminescent and flexible displays; in medicine, for fabrication new kinds of drug delivery systems, for the visualization and monitoring of biological cells, especially for the detecting of the cancerous cell, where the introduction of less toxic GNPs are more desirable than silver NPs; in photodynamic therapy, to kill the tumor cells, germs and viruses, etc.

References

[1] L. de Sio, U. Cataldi, A. Guglielmelli, Th. Burgi, N. Tabiryan, T. J. Bunning. Dynamic optical properties of gold nanoparticles / cholesteric liquid crystal arrays. MRS Commun., 2018, DOI: 10.1557/mrc.2018.80, 1- 6.

[2] J. Li, Z. Lou. Synthesis and applications of gold nanoparticles. In: Importance and Applications of Nanotechnology, 5, 2020, MedDocs Publ., Ch. 2, 8-15.

[3] M.-Ch. Daniel, D, Astruc. Gold nanoparticles: Assembly, supramolecular chemistry, quantum-size-related properties, and applications toward biology, catalysis, and nanotechnology, Chem. Rev., 2004, 104, 293-346.

[4] D. Chenthamara, S. Subramaniam, S. G. Ramakrishnan, S. Krishnaswamy, M. M. Essa, F.-H. Lin, M. Walid Qoronfleh. Therapeutic efficacy of nanoparticles and routes of administration. Biomater. Res. 2019, 23, 1, 20, 1-29.

 https://doi.org/10.52340/ns.2022.12

[5] A. Seaton, L. Tran, R. Aitken, K. Donaldson. Nanoparticles, human health hazard and regulation. J. Royal Soc. Interface, 2010, 7, S1, 119-129.
[6] M. Jasiurkowska–Delaporte, L. Kolek. Nematic liquid crystals. Crystals, 2021, 11(4), 381, 1-2.
[7] A. Choudhary, G. Singh, A. M. Biradar. Advances in gold nanoparticle-liquid crystal composites. Nanoscale, 2014, 6, 7743-7756.
[8] H. K. Bisoyi, S. Kumar. Liquid-crystal nanoscience: An emerging avenue of soft self-assembly. Chem. Soc. Rev., 2011, 40, 306-319.
[9] A. Acreman M. Kaczmarek, G. d'Alessandro. Gold nanoparticle liquid crystal composites as a tunable nonlinear medium. Phys. Rev. E, 2014, 90, 012504, 1-8.
[10] S. H. Sun, C. B. Murray, D. Weller, L. Folks, A. Moser. Monodisperse FePt nanoparticles and ferromagnetic FePt nanocrystal superlattices. Science, 2000, 287, 5460, 1989-1992.
[11] N. Toshima, M. Harada, Y. Yamazaki, K. Asakura. Catalytic activity and structural analysis of polymer-protected gold-palladium bimetallic clusters prepared by the simultaneous reduction of hydrogen tetrachloroaurate and palladium dichloride. J. Phys. Chem., 1992, 96, 24, 9927-9933.
[12] Q. Zhang, J. Y. Lee, J. Yang, Ch. Boothroyd, J. Zhang. Size and composition tunable Ag–Au alloy nanoparticles by replacement reactions. Nanotechnology, 2007, 18, 245605, 1-8.
[13] A. Kumar, J. Prakash, D. S. Mehta, A. M. Biradar, W. Haase. Enhanced photoluminescence in gold nanoparticles doped ferroelectric liquid crystals. Appl. Phys. Lett., 2009, 95, 023117, 1-3.
[14] S.-C. Jeng, C.-W. Kuo, H.-L. Wang, C.-C. Liao. Nanoparticles-induced vertical alignment in liquid crystal cell. Appl. Phys. Lett., 2007, 91, 061112, 1-3.
[15] F. Li, O. Buchnev, C. I. Cheon, A. Glushchenko, V. Reshetnyak, Y. Reznikov, T. J. Sluckin, J. L. West. Orientational coupling amplification in ferroelectric nematic colloids. Phys. Rev. Lett., 2006, 97, 147801, 1-4.
[16] M. Baginski, M. Tupikowska, G. Gonzalez–Rubio, M. Wojcik, W. Lewandowski. Shaping Liquid crystals with gold nanoparticles: Helical assemblies with tunable and hierarchical structures via thin-film cooperative interactions. Adv. Mater., 2019, 32, 1904581, 1-11.
[17] W. Lee, C.-Y. Wang, Y.-C. Shih. Effects of carbon nanosolids on the electro-optical properties of a twisted nematic liquid-crystal host. Appl. Phys. Lett., 2004, 85, 4, 513-515.
[18] S.-J. Hwang, S.-C. Jeng, C.-Y. Yang, C.-W. Kuo, C.-C. Liao. Characteristics of nanoparticle-doped homeotropic liquid crystal devices. J. Phys. D, 2009, 42, 025102, 1-6.
[19] W.-Z. Chen, Y.-T. Tsai, T.-H. Lin. Photoalignment effect in a liquid-crystal film doped with nanoparticles and azo-dye. Appl. Phys. Lett., 2009, 94, 201114, 1-3.
[20] G. Petriashvili, K. Japaridze, L. Devadze, Ts. Zurabishvili, N. Sepashvili, N. Ponjavidze, M. P. de Santo, M. A. Matranga, R. Hamdi, F. Ciuchi, R. Barberi. Paper like cholesteric interferential mirror. Opt. Express, 2013, 21, 18, 20821-20830.
[21] S. Merabia, S. Shenogin, L. Joly, P. Keblinski, J.-L. Barrat. Heat transfer from nanoparticles: A corresponding state analysis. Proc. Natl. Acad. Sci., 2009, 106, 36, 15113-15118.
[22] V. Amendola, R. Pilot, M. Frasconi, O. M. Marago, M. A. Iati. Surface plasmon resonance in gold nanoparticles: A review. J. Phys. Cond. Matter, 2017, 29, 203002, 1-49.

[23] K. George Thomas, P. V. Kamat. Chromophore functionalized gold nanoparticles. Acc. Chem. Res., 2003, 36, 888-898.

[24] J. R. Lakowicz. Principles of Fluorescence Spectroscopy, 2006, New York, Springer, 1-938.

 https://doi.org/10.52340/ns.2022.12